Transverse Characteristics of Short-Pulse Laser-Produced Ion Beams: A Study of the Acceleration Dynamics

E. Brambrink,[1,2,3,*] J. Schreiber,[4] T. Schlegel,[2,3] P. Audebert,[1] J. Cobble,[5] J. Fuchs,[1,6] M. Hegelich,[5] and M. Roth[2,3]

[1]*Laboratoire pour l'Utilisation des Lasers Intenses (LULI) Unité Mixte n° 7605 CNRS - CEA - Ecole Polytechnique - Université Pierre et Marie Curie, Ecole polytechnique, Palaiseau, France*

[2]*Institute for Nuclear Physics, Darmstadt University of Technology, Darmstadt, Germany*

[3]*Gesellschaft für Schwerionenforschung, Darmstadt, Germany*

[4]*LMU, München, Germany*

[5]*Los Alamos National Laboratories, Los Alamos, New Mexico, USA*

[6]*Nevada Terawatt Facility, University of Nevada, Reno, Nevada, USA*

(Received 19 January 2006; published 21 April 2006)

We report on first measurements of the transverse characteristics of laser-produced energetic ion beams in direct comparison to results for laser accelerated proton beams. The experiments show the same low emittance for ion beams as already found for protons. Additionally, we demonstrate that the divergence is influenced by the charge over mass ratio of the accelerated species. From these observations we deduced scaling laws for the divergence of ions as well as the temporal evolution of the ion source size.

DOI: 10.1103/PhysRevLett.96.154801 PACS numbers: 29.27.Fh, 52.38.Kd, 52.40.Kh

Introduction.—Energetic ions, emitted from solid density targets during the interaction with ultraintense lasers, are an interesting area of research *per se*, but also exciting because of the various possibilities of applications [1–3]. Intense proton beams, observed in several laboratories [4–6], are collimated (divergence angle $<20°$), carry high currents (MA), and reach energies up to 50 MeV. Many experiments have been performed to investigate the influence of target [7–9] and laser parameters [10,11] on the proton beam characteristics to understand the acceleration mechanisms.

The acceleration of ions with lasers is complementary to that of energetic protons. Because of their specific interaction characteristics (higher stopping power, different nuclear reaction), ion beams may be in favor for several applications, e.g., isochoric heating, isotope production, or the injection into a conventional accelerator. Moreover, the latter applications will strongly profit from the high brightness and low emittance of these beams. To make such applications work, it is important to study the characteristics of ion beams in detail and to develop practical scaling laws. Since ions with different masses and charge states will appear at the same time in the space charge volume, the complex acceleration process itself can be analyzed, measuring, for example, the maximum electric field strength [12,13]. In this Letter, we investigated the transverse characteristics of laser-produced light ion beams, from which we concluded on the acceleration dynamics.

For our experimental conditions, the acceleration from the nonirradiated rear surface, so-called target normal sheath acceleration (TNSA) [14,15], is the dominant mechanism [16]. In this model, a beam of energetic electrons is generated during the interaction of the laser with the front surface of the target, propagates through the target, and sets up an electrostatic field (typ. 10^{12} V/m) on the rear surface. This field ionizes all atoms in a surface layer due to field ionization and subsequently accelerates them. Usually, there is a thin layer of impurities present on the target surface containing hydrogen (water, hydrocarbons), thus providing protons for the acceleration. Since the charge over mass ratio for the protons is higher than for all other ion species, the protons undergo the strongest acceleration, ranging out the other species and shielding them from the space charge field, suppressing their acceleration. Removing these contaminants [12,17], the proton generation will be inhibited but the acceleration of ions can be enhanced remarkably. The acceleration of light ions, such as carbon, beryllium, oxygen, or fluorine, as well as heavier species like palladium to high energies has been demonstrated recently [18].

An important discovery for the exploration of the transverse beam parameters of laser generated protons was the possibility of beam intensity profiling by means of spatial structures on the rear surface of the target. With this technique, the source size on the rear surface of the target as well as the beam emittance were determined. The latter result pointed at an extremely laminar expansion [19]. For this Letter, we have extended this technique to light ions studying the corresponding beam parameters.

Experimental setup.—The experiments were performed with the 100 TW laser system of the Laboratoire pour l'Utilisation des Lasers Intenses (LULI). A laser beam with 20 J in 350 fs was focused with an $f/4$ off-axis parabola onto a thin foil providing focal intensities of $2–5 \times 10^{19}$ W/cm^2.

We irradiated 25 μm thick gold and tungsten foils with engraved linear structures of 10 μm spacing on the rear surface. The tungsten foils were heated by a high current up to 1300 °C to remove hydrogen and carbon impurities from the target surface. In this case, we observed that only the stable oxides remained, providing a beam of oxygen ions.

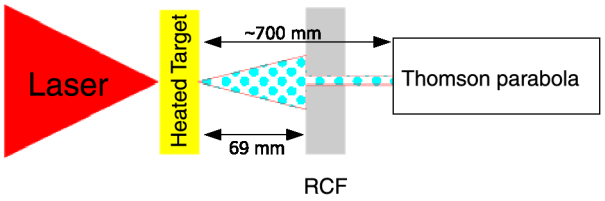

FIG. 1 (color online). Experimental setup. Ions are characterized with a Thomson parabola (spectrally) and with RCF (spatially).

Figure 1 shows the setup for the ion diagnostics used in this experiment. The ions were detected with a Thomson parabola, a spectrometer with parallel magnetic and electric fields, which disperses ions with different q/m values on separate parabolas. The distance between the spectrometer and the target was about 70 cm; the entrance pinhole had a diameter of 200 μm, which corresponds to a solid angle of approximately 3×10^{-8} sr.

The spectrally dispersed ions were detected with a CR-39 plastic detector [20], where the ions cause a local destruction of the polymer structure, which leaves later a small crater (pit) after etching in NaOH. These pits were then counted under a microscope to obtain an energy spectrum.

For the angular distribution measurement of the ions, radiochromic film (RCF) [21] was placed in a distance of 63 mm in front of the entrance pinhole of the Thomson parabola. This film is sensitive to the deposition of energy by ionizing radiation. As the energy deposition of the ions is very high in comparison to electrons and x rays, the imprint in this detector is mainly caused by ions.

Experimental results.—Figure 2 shows a spectrum obtained with the Thomson parabola for the charge state $Z = 6+$ of oxygen, which was the highest charge state measured in this experiment. Only the ions of this charge state

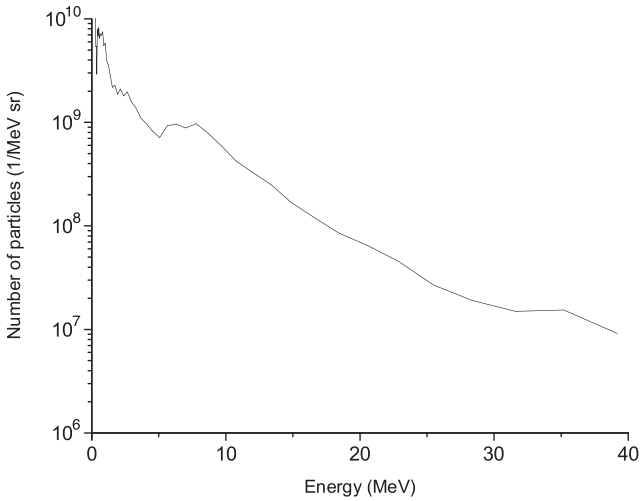

FIG. 2. Energy spectrum for the O6+ ions obtained with the Thomson parabola spectrometer.

are energetic enough to be compared with protons; the lower charge states are therefore disregarded. The spectrum shows an exponential energy distribution with a mean energy (temperature) of 5 MeV, which was also deduced from the RCF stack for a proton beam from an unheated target under the same experimental conditions. The spectrum obtained from the Thomson parabola ensured also the absence of protons which could have falsified the results obtained with RCF. The resemblance between ions and protons concerning laser parameters and spectral characteristics allows us to assume the same accelerating field and to compare the transverse parameters directly.

From the beam profiles obtained with the RCF detectors, we deduced the divergence of the beam and the size of the ion source on the rear surface of the target. Since each layer of the RCF stack detects a different group of ions with an energy, at which those ions are stopped (highest deposition in the Bragg peak), these parameters can be measured for several particle energies in the case of protons. However, for heavy ions due to their low penetration depth, this is possible only for one distinct energy, which is determined by the protective aluminum layer (13 μm thick) in front of the RCF. In our case, this total energy was $\approx$16.5 MeV, which corresponds to an acceleration potential (equivalent proton energy) of 2.75 MeV for the measured charge state O6 + . The ions with lower charge states are stopped in the protective layer.

In Fig. 3, the source size and the divergence for protons and ions are plotted over the accelerating potential. For the proton beam, we see a linear dependence of the source size on the potential and a divergence, which is proportional to the source size. These findings correspond well to the results in Ref. [19] and have also been observed systematically over a wide range of experimental conditions and

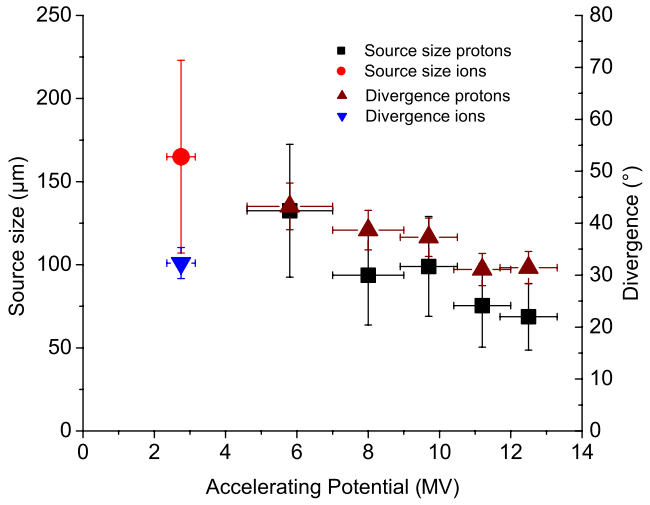

FIG. 3 (color online). Source size and divergence (foot-to-foot) measured for different accelerating potentials. While the source size has comparable values for ions and protons, the divergence for ions is significantly lower.

proton energies [22]. The source size obtained for the heavy ions fits well into the linear dependence found for the protons, while the divergence is significantly lower, about a factor of 1.6. Also the magnification of the structure on the rear surface of the target is decreased by the same factor; the beam divergence is therefore changing globally and not only at the edge of the beam.

Furthermore, the intensity modulation of the beam allows us to measure the transverse beam emittance. Following the approach of Ref. [19], we obtain a normalized emittance of 0.09 mm mrad, which is close to that for protons and much lower than for conventional ion sources [e.g., 2.5 mm mrad for the GSI UNILAC accelerator [23]].

Discussion.—The measurement of the transverse beam parameters of heavy ions reveals many similarities between the acceleration of protons and heavy ions. Ions as well as protons are emitted from the cold rear surface, resulting in a low-emittance, laminar beam. The spatial distribution of the acceleration potential is independent of the accelerated ion species, as suggested by the measurements of the source size. This is consistent with the TNSA model, which considers an electric field determined by the (spatial) electron distribution.

However, the divergence of the heavy ion beam is significantly lower than the proton beam divergence, which can be explained by the lower velocity of ions compared to that of protons after passing the same acceleration potential. The divergence is directly related to the shape of the ion front in the beginning of the free propagation, which can be well approximated by an inverse parabola [24], and is only determined by the diameter and the maximum of this parabola, e.g., the maximum distance of the ion front from the initial surface (see Fig. 4). Since the parabola is defined by the source size and the divergence, we can estimate a corresponding distance of ≈ 12 μm for the ion front, which is 1.6 times smaller than for protons under equivalent experimental conditions.

Since the ions detected in a distinct layer of the RCF have all the same energy, the final velocity of these ions is the same. Therefore, the curvature of the ion front cannot be explained by different ion velocities at the central part of the beam and on its edge. We attribute this curvature to a temporal effect in the ion acceleration, where the ions at the edge start later in time than in the middle of the acceleration field. So, the distance between the ion front in the center of the beam and the initial target surface should scale with the ion sound velocity c_s, which can be described analytically in an isothermal one-dimensional expansion approximation [25]:

$$c_s = \sqrt{\frac{Zk_BT}{m_i}} \propto \sqrt{\frac{Z}{m_i}}. \tag{1}$$

Here T is the electron temperature, Z the charge state of the ion, m_i the ion mass, and k_B the Boltzmann constant. For the oxygen ions we calculate an ion sound velocity, which is $\sqrt{16/6} = 1.63$ times smaller than for protons. This value matches very well the measured one.

From the model we can estimate the time delay in the beam propagation between the beam edge and at its center. With an electron temperature of 2 MeV [26], the sound velocity c_s is 8.5×10^6 m/s and the delay becomes 1.4 ps, which is in agreement with radiography experiments [27], showing the expansion of the whole ion front within the first two ps.

Finally, it is possible to evaluate the temporal evolution of the ion source size. With the parabolic shape for the ion front $y = y_f(t) - x^2$ (see Fig. 4), we find for the source size on the target $r^2(t) = y_f(t) \propto \langle c_s \rangle t$ and arrive at the following expressions for the temporal evolution and the growth rate of the source size:

$$r(t) = r_0\sqrt{\frac{t}{t_0}}, \qquad \dot{r}(t) = \frac{r_0}{2t_0}\sqrt{\frac{t_0}{t}}, \tag{2}$$

where r_0 and t_0 are fit parameters, which can be calculated from a measured source size and divergence. In our experiment we obtained the values $r_0 \approx 83$ μm and $t_0 \approx 1.4$ ps. Figure 5 shows the growth rate of the ion source. The initial source size radius, defined by the focal spot and the divergence of the electron beam inside the target [28], is ≈ 20 μm; therefore, this model is only valid for times $t > 120$ fs. Measurements of the rear side reflectivity [29] show qualitatively the same temporal dependence (hyperbolic) but different values for the maximum velocity, which can be attributed to the different laser intensity in those experiments.

The initial growth rate can be well explained if one suggests that the electrons gain a transverse momentum in a self-generated field on the rear surface (fountain effect) [30]. We estimated the transverse velocity predicted by this model. An electron, traveling at the speed of light with the momentum p, gains the transverse velocity,

$$v_t = \frac{cl}{R}, \qquad R = \frac{pc}{eB}, \tag{3}$$

while traveling through a magnetic field B of length l. With

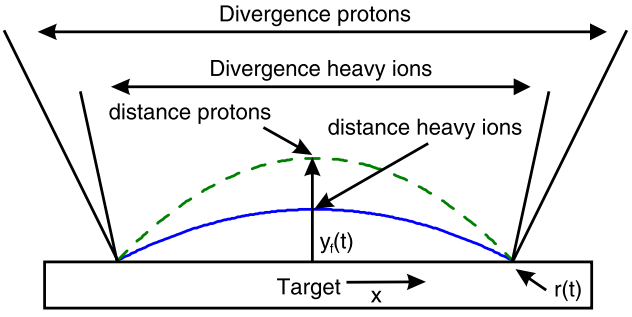

FIG. 4 (color online). Illustration of the correlation between beam divergence and the curvature of the ion front, which depends on the expansion velocity in the center of the beam.

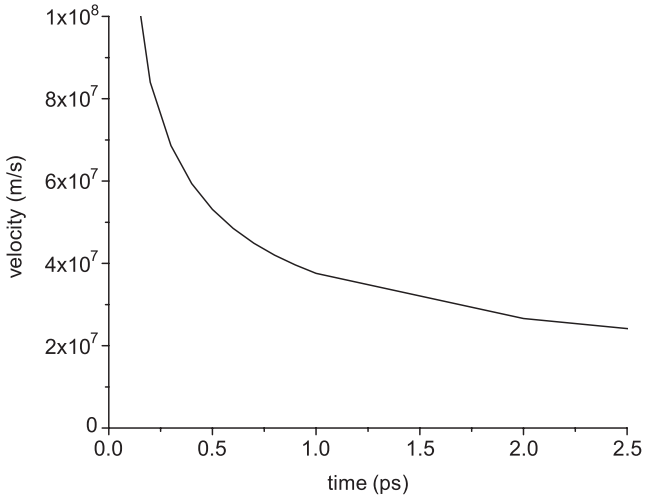

FIG. 5. Growth rate of the ion source deduced from the source size and divergence measurements for heavy ions.

$B = 1000$ T [30], $l = 2$ μm (Debye length) and an electron energy of 2 MeV we obtain a v_t of approximately 8×10^7 m/s, which is close to the values shown in Fig. 5.

Summary.—We have measured for the first time the transverse characteristics of laser-produced ion beams and compared those to results for protons obtained under similar experimental conditions. We demonstrated an excellent ion beam quality (e.g., low emittance) similar to laser generated proton beams. This is an important result for future applications, where a good focusability and/or beam quality is essential. Especially for the future accelerator development aiming for ultrabright beams, short-pulse laser based ion sources can be a key component.

The size of the emitting area on the rear surface as well as the electric field distribution is comparable to values obtained for protons. The significantly lower divergence can be explained by the influence of the higher ion mass on the acceleration dynamics resulting in an emission angle scaling with the ion sound velocity.

Thus for the design of post acceleration and beam guiding, the results obtained for protons, which afford less sophisticated experiments, can be scaled to various ion species. In addition, we got some insight into the dynamics of the beam generation, examining the temporal evolution of the ion emitting zone on the rear surface.

We thank the staff of the LULI laser for their ongoing help during the experiment and the ''Institut für Halbleitertechnik'' at Darmstadt for target preparation. This work was supported by the Grant No. E1127 from Région Ile-de-France and by BMBF.

*Electronic address: erik.brambrink@polytechnique.fr

[1] M. Roth *et al.*, Phys. Rev. Lett. **86**, 436 (2001).
[2] M. Borghesi *et al.*, Laser Part. Beams **20**, 269 (2002).
[3] I. Spencer *et al.*, Nucl. Instrum. Methods Phys. Res., Sect. B **183**, 449 (2001).
[4] A. Maksimchuk, S. Gu, K. Flippo, D. Umstadter, and V. Yu. Bychenkov, Phys. Rev. Lett. **84**, 4108 (2000).
[5] R. A. Snavely *et al.*, Phys. Rev. Lett. **85**, 2945 (2000).
[6] E. L. Clark *et al.*, Phys. Rev. Lett. **84**, 670 (2000).
[7] M. Roth *et al.*, Phys. Rev. ST Accel. Beams **5**, 061301 (2002).
[8] M. Kaluza *et al.*, Phys. Rev. Lett. **93**, 045003 (2004).
[9] A. J. Mackinnon *et al.*, Phys. Rev. Lett. **88**, 215006 (2002).
[10] Y. Oishi *et al.*, Phys. Plasmas **12**, 073102 (2005).
[11] J. Fuchs *et al.*, Nature Phys. **2**, 48 (2006).
[12] M. Hegelich *et al.*, Phys. Rev. Lett. **89**, 085002 (2002).
[13] J. Schreiber *et al.*, Appl. Phys. B **79**, 1041 (2004).
[14] S. P. Hatchett *et al.*, Phys. Plasmas **7**, 2076 (2000).
[15] S. C. Wilks *et al.*, Phys. Plasmas **8**, 542 (2001).
[16] J. Fuchs *et al.*, Phys. Rev. Lett. **94**, 045004 (2005).
[17] M. Allen *et al.*, Phys. Rev. Lett. **93**, 265004 (2004).
[18] M. Hegelich *et al.*, Phys. Plasmas **12**, 056314 (2005).
[19] T. E. Cowan *et al.*, Phys. Rev. Lett. **92**, 204801 (2004).
[20] A. P. Fews, Nucl. Instrum. Methods Phys. Res., Sect. B **71**, 465 (1992).
[21] W. L. McLaughlin *et al.*, Nucl. Instrum. Methods Phys. Res., A **302**, 165 (1991).
[22] E. Brambrink *et al.*, Europhys. Conf. Abstr. **29C**, P-2.163 (2005).
[23] W. Barth *et al.*, *Proceedings EPAC 2004* (European Physical Society Accelerator Group, Lucerne, Switzerland, 2004), p. 1171.
[24] E. Brambrink, A. Blazevic, M. Roth, and T. Schlegel, Laser Part. Beams **24**, 163 (2006).
[25] P. Mora, Phys. Rev. Lett. **90**, 185002 (2003).
[26] M. Allen *et al.*, Phys. Plasmas **10**, 3283 (2003).
[27] L. Romagnani *et al.*, Phys. Rev. Lett. **95**, 195001 (2005).
[28] J. J. Santos *et al.*, Phys. Rev. Lett. **89**, 025001 (2002).
[29] E. Martinolli *et al.*, Phys. Rev. E **70**, 055402(R) (2004).
[30] A. Pukhov, Phys. Rev. Lett. **86**, 3562 (2001).